LBL-30635

Lawrence Berkeley Laboratory
UNIVERSITY OF CALIFORNIA

Physics Division

Invited talk presented at the Rencontres de Physiques de la
Valle d'Aosta, La Thuile, Italy, March 4–9, 1991,
and to be published in the Proceedings

Physics Possibilities at LHC/SSC

I. Hinchliffe

April 1991

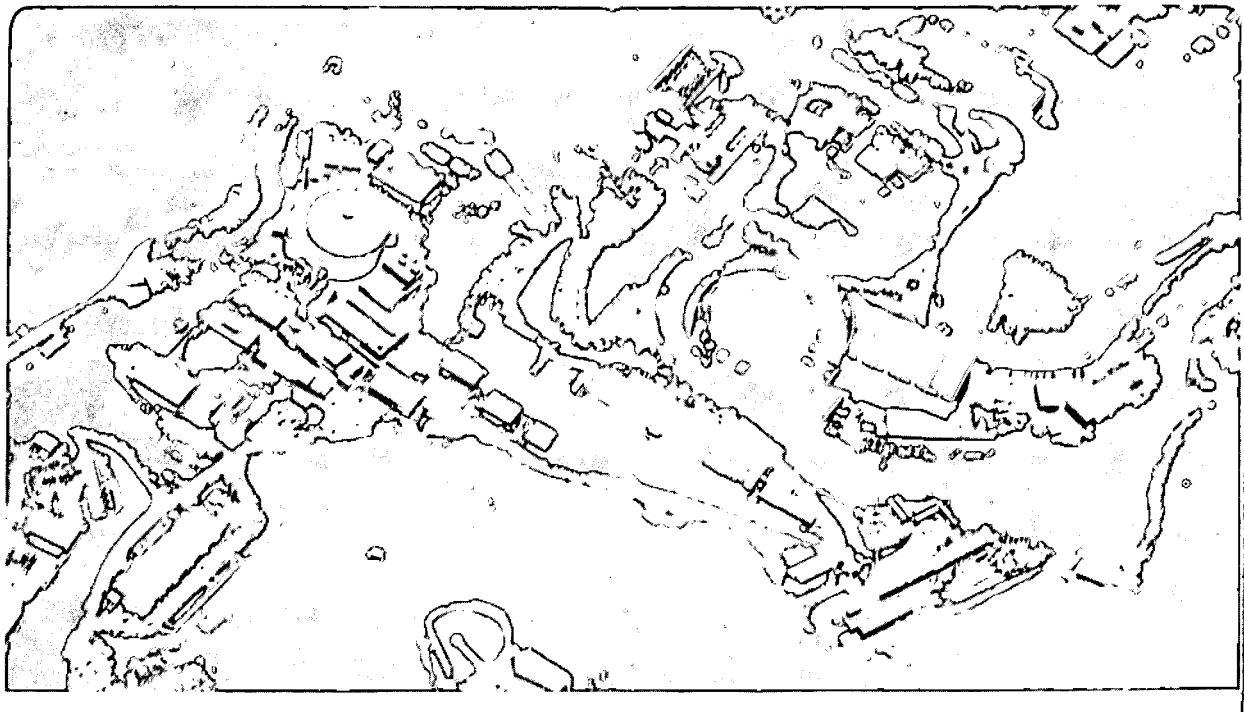

Prepared for the U.S. Department of Energy under Contract Number DE-AC03-76SF00098

DISCLAIMER

April 25, 1991 LBL-30635

Physics Possibilities at LHC/SSC *

Ian Hinchliffe

Theoretical Physics Group
Physics Division
Lawrence Berkeley Laboratory
1 Cyclotron Road
Berkeley, California 94720

Abstract

I review some recent work on physics simulations for SSC/LHC.

In this talk, I review some of the recent developments in physics simulations for the SSC/LHC and comment upon the requirements that are placed upon detectors by the need to extract specific physics signatures. I shall draw upon the material in the various EOI/LOI documents[1-6] submitted to the SSC Laboratory and upon the work done at the Aachen LHC workshop.[7] In the following discussion 1 SSC (LHC) year corresponds to an integrated luminosity of 10 (100) fb^{-1}.

Invited talk given at the "Rencontres de Physiques de la Vallee d'Aosta", La Thuile, Italy March 4-9 1991.

*This work was supported by the Director, Office of Energy Research, Office of High Energy and Nuclear Physics, Division of High Energy Physics of the U.S. Department of Energy under Contract DE-AC03-76SF00098.

The standard Model Higgs boson.

This has become a benchmark process and any multipurpose SSC/LHC detector must be able to find it. It is convenient to divide the possible Higgs mass into three ranges:- (a) $80GeV \lesssim M_H \lesssim 2M_Z$, (b) $2M_Z \lesssim M_H \lesssim 750GeV$ and (c) $M_H \gtrsim 750GeV$. I will assume that a Higgs of mass less than 80 GeV will have been found at LEP before the hadron colliders are available.

The region (b) is the simplest. One looks in the channels $H \rightarrow ZZ \rightarrow e^+e^-e^+e^-$, $e^+e^-\mu^+\mu^-$ and $\mu^+\mu^-\mu^+\mu^-$. Each pair of dileptons is required to have an invariant mass consistent (within experimental resolution) with the Z mass. A detector with modest resolution such as SDC[1,4] which has an iron toroid muon system, is capable of extracting the signal. The background arises from the processes $gg \rightarrow ZZ$ [8] and $q\bar{q} \rightarrow ZZ$ [9]. There is a very small additional background arising from the final states $t\bar{t}$, $Z + t\bar{t}$ and $Z + b\bar{b}$ where the leptons arise from the semi-leptonic decay of heavy quarks; this is negligible once we require that there be two pairs of leptons with mass $M_Z \pm 10GeV$. Even for a Higgs mass of 800 GeV the resolution afforded by an iron toroid system is good enough to ensure that such a cut can be made with good efficiency. Figure 1 shows the reconstruction in this channel with $M_H = 400$ GeV.

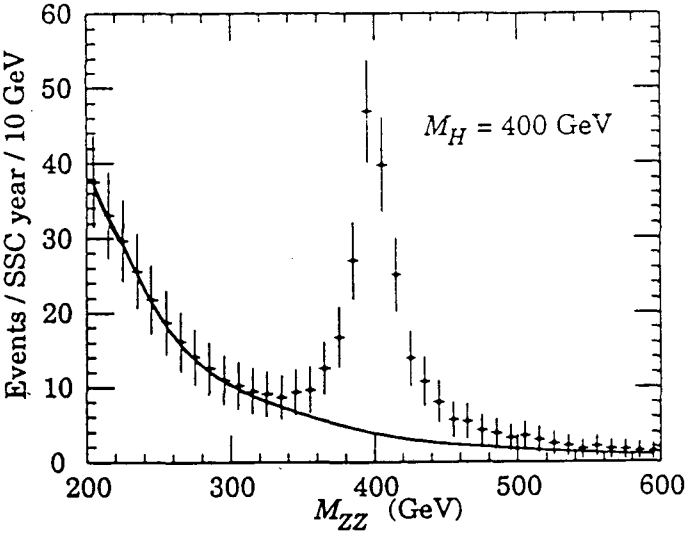

Figure 1 The ZZ invariant mass distribution showing a peak due to a Higgs of mass 400 GeV in the final states $e^+e^-e^+e^-$, $\mu^+\mu^-e^+e^-$, $\mu^+\mu^-\mu^+\mu^-$. Two of the leptons (the trigger) are required to have

$p_t > 20$ GeV and the other two are required to have $p_t > 10$ GeV. All leptons have $|y| < 2.5$ and an efficiency factor of 0.65 has been applied. The two lepton pairs were both required to have $M_{\ell\ell} = M_Z \pm 10$ GeV. The backgrounds curves are cumulative, and are (from lowest to highest): $q\bar{q} \rightarrow ZZ$, multiplied by 1.65 to account for $gg \rightarrow ZZ$, $Z + b\bar{b}$, $Z + t\bar{t}$, and $t\bar{t}$. But the ZZ background gives the only visible contribution. Figure from References 4 and 10.

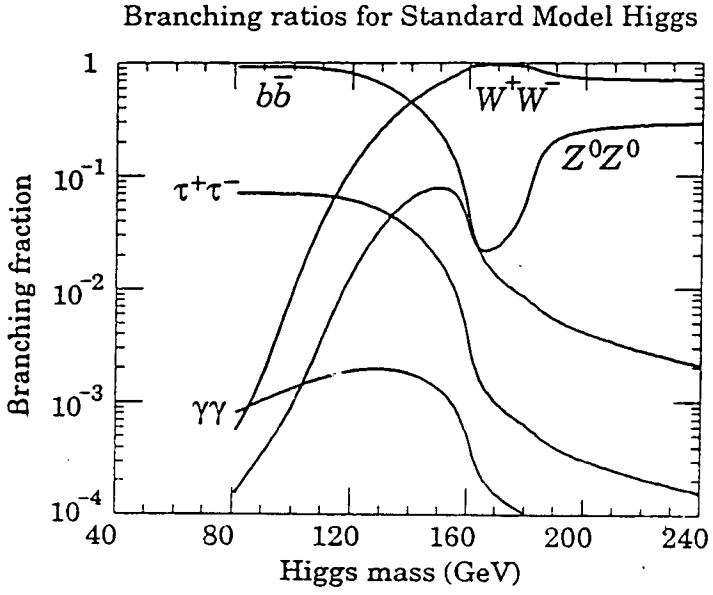

Figure 2 The branching ratio for a Higgs boson into various channels as a function of its mass.

In region (a) the situation is more complicated. Figure 2 shows the branching ratio of a Higgs boson into various channels as a function of its mass. The only channels that have acceptable signal to background are ZZ^* with its subsequent decay to four charged leptons (Z^* indicates an off mass shell Z boson) or $\gamma\gamma$. The decay to $\tau\tau$ [11] has been investigated in some detail and found not to be viable[12]. There is a minimum mass or order 125 GeV below which the ZZ^* mode is not useful. The branching ratio falls very rapidly below this value, so that an increase of the integrated luminosity of an experiment is not effective. In addition, the mean transverse momentum of the decay leptons falls leading to a loss of efficiency[10]. There is now only one Z in the final state and the loss

of the Z mass constraint on the second pair of leptons causes an increase in the background over that shown in Figure 1. In particular the background from $t\bar{t}$ is quite large unless we require that the leptons be isolated: *i.e.* that there be less than 5 GeV of additional energy in a cone of radius $\Delta R = 0.3$ around the lepton direction. This isolation criterion reduces the rate of leptons arising from b and c decay. In figure 3, the rate for such leptons has been reduced by a factor of 10 to account for isolation. This factor is conservative, a larger factor is readily obtainable[10].

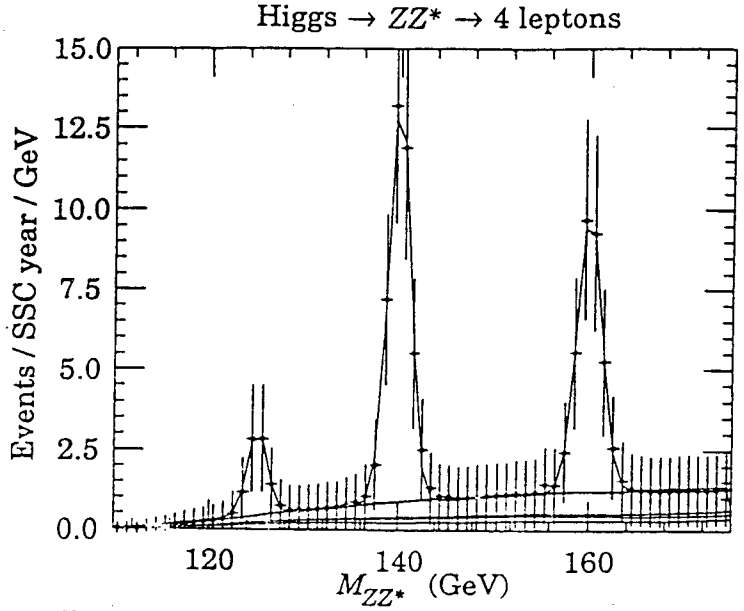

Figure 3 The reconstructed Higgs mass for ZZ^* decaying to $4e$, 4μ, and $2e2\mu$ with $M_H = 125, 140, 160$ GeV, including the expected backgrounds. The backgrounds curves are cumulative, and are (from lowest to highest): $q\bar{q} \rightarrow ZZ^*$, multiplied by 1.65 to account for $gg \rightarrow ZZ^*$, $Z + b\bar{b}$, $Z + t\bar{t}$, and $t\bar{t}$. Figure from ref. 4.

The decay $H \rightarrow \gamma\gamma$ is to be observed over the background from $q\bar{q} \rightarrow \gamma\gamma$ and $gg \rightarrow \gamma\gamma$ (the latter is dominant). There is an additional background that arises from $jet - jet$ or $jet - \gamma$ final states where the jet fragments in such a way that it produces an isolated π^0 that is indistinguishable from a photon. A rejection factor of 10^{-4} for each jet is needed to reduce these backgrounds below the continuum $\gamma\gamma$ rate. Rejection factors of less than 10^{-3} have already been achieved at UA2[13] and CDF[14]. A resolution in the $\gamma\gamma$ mass of 1% or better is needed in order to ensure that a signal can be extracted above the $\gamma\gamma$ background

for Higgs masses above 80 GeV. In order to achieve such resolution, the position of the event vertex along the beam direction must be known to 5mm. Since the average number of events per crossing is (much) greater than one at SSC (LHC), a method of assigning the event to a primary vertex is needed. Choosing the event with the highest multiplicity will be the correct choice on average. Figure 4 taken from the L* LOI[6] shows the resulting $\gamma\gamma$ spectrum after subtracting the smooth background. The background from $jet-\gamma$ and $jet-jet$ is not included. An electromagnetic resolution of $1.3\%/\sqrt{E}+0.5\%$ is assumed. (Here E is in GeV.) For masses between 100 and 160 GeV a peak can clearly be seen. At lower mass the statistical significance of the signal is less. The signal is only slightly degraded if the resolution is relaxed to $7.5\%/\sqrt{E}+0.5\%$ [5].

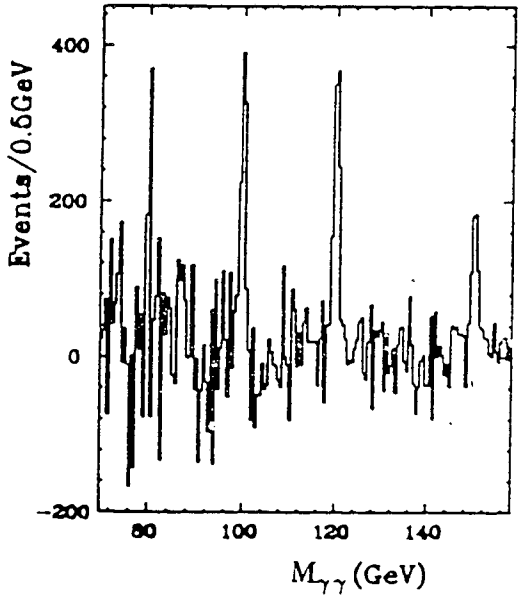

Figure 4 The $\gamma\gamma$ spectrum after background subtraction. The peaks correspond to Higgs masses of 80, 100,120 and 150 GeV. The photons are required to have $|\eta| < 2.8$ and $E_T > 20$ GeV. In addition the $\gamma\gamma$ system is required to have $|\eta| < 3$ and the angle (θ^*) between either photon and the direction of the pair measured in the center of mass frame of the pair is required to satisfy $|\cos\theta^*| < 0.8$. Figure from ref. 6, for SSC.

If the Higgs boson is produced in association with a W from the processes $q\bar{q} \rightarrow H+W$ or $gg \rightarrow t\bar{t}H$ then the signal to background ratio is somewhat larger and so a less stringent requirement is imposed on the calorimeter resolution. Furthermore the presence of the $W(\rightarrow \ell\nu)$ enables the vertex to be located unambiguously. The signal and background have been analysed in detail in the case of $q\bar{q} \rightarrow WH \rightarrow \gamma\gamma\ell\nu$ [4,5,15]. Backgrounds were included from final states of 3-jets, $2-jet+\gamma$, $jet+\gamma\gamma$, $b+\gamma\gamma$, $b+\gamma+jet$, $b\bar{b}+\gamma$, $W+\gamma+jet$ and $W+\gamma\gamma$. Isolation cuts on the leptons arising from b-quark decay were assumed to reduce the rate of such leptons by a factor of 10 (see above). In addition the probability that a light quark jet could fake an electron or photon was assumed to be 5×10^{-4}. The dominant background is then from the $W\gamma\gamma$ final state. Figure 5 shows the resulting $\gamma\gamma$ invariant mass distribution with peaks corresponding to Higgs masses of 80, 100, 120 and 140 GeV. The SDC photon resolution of $15\%/\sqrt{E}+1\%$ is assumed.

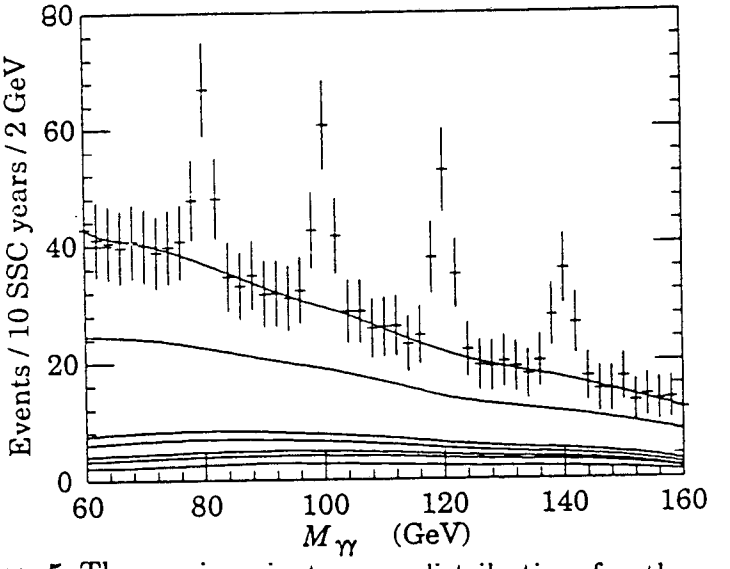

Figure 5 The $\gamma\gamma$ invariant mass distribution for the process $q\bar{q} \rightarrow WH \rightarrow \ell\nu\gamma\gamma$. The background curves are cumulative and are (from lowest to highest) from $3-jet$, $2-jet+\gamma$, $jet+\gamma\gamma$ (combined), $b+\gamma\gamma$, $b+\gamma+jet$, $b\bar{b}+\gamma$, $W+jets$, $W+\gamma+jets$, and $W\gamma\gamma$. The photons and lepton are all required to have $p_t > 20$ GeV and $|\eta| < 2.5$ and to be separated from each other by $\Delta R > 0.4$. Figure from ref. 15 for SSC. Including the $t\bar{t}H$ final state will increase the signal in the peaks by approximately a factor of 6.

The rate of $\ell\gamma\gamma$ arising from the $t\bar{t}H$ is about 6 (2) times larger than that from $q\bar{q} \rightarrow WH$ at SSC (LHC)[16]. This factor is roughly independent of the top quark mass for top masses between 100 and 200 GeV. The signal events are busier than those from the WH final state since they have 2 additional b—quarks and a W. This extra complexity may result in a slight loss of efficiency but will help in reducing the background shown in Figure 5 still further. It is now clear that the SSC operating at 10^{33} cm^{-2} sec^{-1} or an LHC operating at 10^{34} cm^{-2} sec^{-1} design luminosity should be able to find a Higgs boson if its mass lies in region (a) and that a detector with extraordinary electromagnetic energy resolution is not required.

In region (c) there are two problems: lack of rate and a signal with no clear peak. In order for a Higgs boson to have a mass of more than 800 GeV in the standard model, the self coupling and consequently the coupling to W and Z bosons must become large. Hence the width of the Higgs boson becomes very big ($\Gamma_H \sim 500GeV(\frac{M_H}{1TeV})^3$) and the well defined peak in the ZZ invariant mass as lower values of the Higgs mass disappears. More serious is that we loose the only tool (perturbation theory) that we have for reliably calculating rates.

Scalar field theories, such as the Higgs sector of the standard model, that have non-zero couplings can only be effective theories valid over a limited range of energies[17], up to some energy scale Λ . If we require that $\Lambda \sim M_{Planck}$, the scale where gravitational interactions of elementary particles become important then the Higgs mass must be less than 125 GeV or so. Requiring that $\Lambda > M_H$ so that the theory is sensible on scales up the Higgs mass itself implies that $M_H \lesssim 800$ GeV. These constraints are not valid if new physics is added to the standard model. For example, in supersymmetric theories the Higgs self coupling is determined by gauge interactions and does not increase with the mass of the Higgs[18]. In technicolor theories[19], there are no elementary scalars, the role of the Higgs bosons is played by fermion-antifermion bound states, and the above considerations are inapplicable.

In general, one should search for some structure in final states of pairs of gauge bosons and I will now give some examples. A standard model Higgs boson of mass 800 GeV is probably close to the limit of what is allowed. Figure 6 shows the signal in the case of the ZZ final state where the Z's decay to e^+e^- or $\mu^+\mu^-$. The statistical significance of the signal is poor and the "peak" is very broad. It

may be possible to include the final states where one Z decays to $\tau^+\tau^-$ [5]. The direction of the tau's is given by the direction of their decay products; using the Z mass as a constraint then enables the ZZ invariant mass to be reconstructed. Taus are recognised via their decays into low multiplicity jets ($\tau \rightarrow \pi\nu$, $\tau \rightarrow \rho\nu$, $\tau \rightarrow a_1\nu$ *etc.*); there is no significant background.

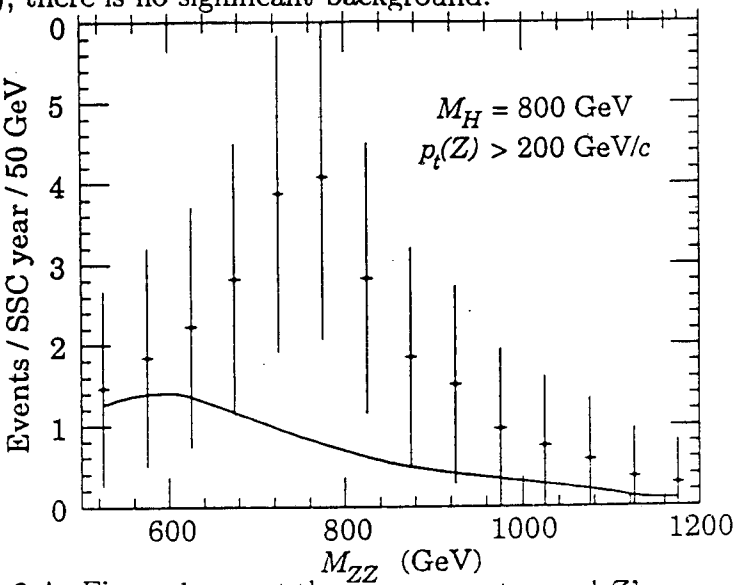

Figure 6 As Figure 1 except that the reconstructed Z's are required to satisfy $p_t > 200$ GeV and $M_H = 800$ GeV. Figure from ref. 10 for SSC.

The issue of simulation of a signal corresponding to a "heavy Higgs boson" is complicated by the absence of unambiguous models with which to predict. One issue in the case of the standard model Higgs concerns the form of the Higgs propagator in the expression for the production rate of Z pairs. This has the form $\frac{1}{(s-M_H^2)^2+\Gamma_H^2 M_H^2}$ where $\sqrt{s}$ is the invariant mass of the ZZ system. The width $\Gamma_H \propto M_H^3$ should be replaced by the imaginary part of the self energy $\Pi(s)$ $(= \Gamma_H(\frac{\sqrt{s}}{M_H})^3)$ in this formula. This replacement is not important at low values of the Higgs mass. At large values it changes the shape of the peak considerably.[20]

In the ZZ final state the ability to establish a signal will depend critically upon the confidence that one has in the expected event rates in the standard model without a heavy Higgs. Since the model with no Higgs boson is not renormalizable and therefore predicts an infinite rate for ZZ production this

background is best estimated from the expected rate using a light ($M_H \sim 100$ GeV) Higgs boson. The ZZ final state receives contributions from $q\bar{q} \rightarrow ZZ$, $gg \rightarrow ZZ$ which proceeds via intermediate states involving quarks and Higgs bosons, and $qq \rightarrow qqZZ$. The rates are calculated according to the usual parton model expression.

$$\sigma = \int dx_1 dx_2 f(x_1, Q^2) f(X_2, Q^2) \hat{\sigma}$$

where $f(x, Q^2)$ are the quark and gluon distribution functions and $\hat{\sigma}$ is the partonic cross section. In order to make a reliable estimate of the rates, the partonic cross section must be known to next to leading order in α_s. Without such knowledge there will be an uncertainty of order 50% in the estimated rates arising from the (arbritrary) choice of Q^2. If the non-leading corrections are known and QCD perturbation theory is reliable, the Q^2 dependence in $f(x, Q^2)$ is partially cancelled by that in $\hat{\sigma}$. At present these non-leading corrections are only known for the $q\bar{q} \rightarrow ZZ$ process[8]. They are not known for the $gg \rightarrow ZZ$ process which contributes approximately 40% to the total ZZ rate[9]. The ZZ rate will be measured at low invariant masses, and these measurements will help to remove some of the uncertainties in the rate expected at high masses. Our present knowledge coupled with these measurements will probably enable this rate to be estimated to 20%.

The statistical significance of the signal can be further improved by using the $ZZ \rightarrow \ell\ell\nu\nu$ final states. Here the invariant mass of the ZZ system cannot be measured but one must look at the event rate as a function of missing transverse energy (E_T). In addition to the backgrounds present in the 4ℓ final states, there are additional backgrounds from $t\bar{t} \rightarrow \ell^+\nu\ell^-\nu + X$ where the $\ell^-\ell^-$ mass is consistent with a Z and from $Z + jets$ where the jet energies are mismeasured to give rise to an apparent missing E_T. The former background is not serious. In order to control the latter the detector must be hematic with calorimeter coverage extending to $|\eta| < 5$ at SSC and $|\eta| < 4.5$ at LHC. Figure 7 shows the distribution in missing E_T. Events are rejected if they contain a jet with $E_t > 300$ GeV. This cut has no effect on the signal but is used to reject the $Z+jets$ background that arises when a jet's energy is substantially mismeasured. If the jet energy resolution is gaussian, this background is irrelevant and the cut can be dropped. However, in the simulation used to produce this figure, the jet energy resolution has a very substantial non-Gaussian tail[21] modeled on that

observed in CDF which is due principally to ϕ-cracks[22].

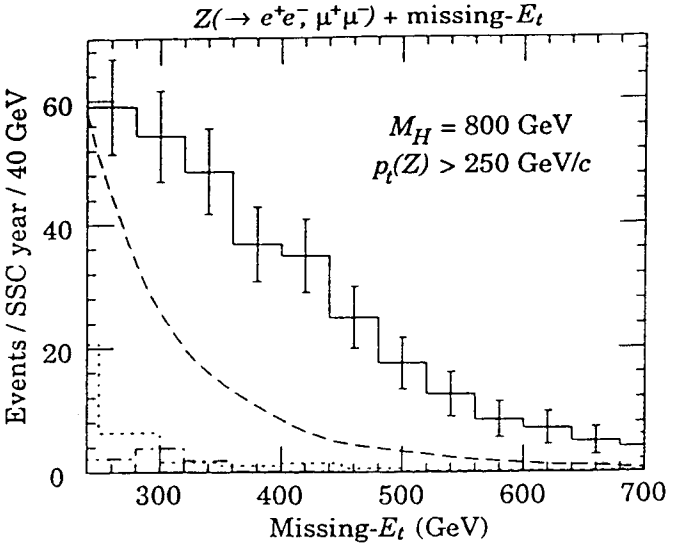

Figure 7 The distribution (solid histogram) in missing E_T for the final state $Z(\rightarrow \mu^+\mu^-, e^+e^-)$+ missing E_T including the effect of a Higgs boson of mass 800 GeV and the various backgrounds. The reconstructed Z is required to have $p_T > 250$ GeV and the events are rejected if they contain a jet with $E_T > 300$ GeV. For clarity, the figure shows the separate components of the background. The background shown as a dashed curve arises from $q\bar{q} \rightarrow ZZ$ (multiplied by 1.65 to account for the $gg \rightarrow ZZ$ process). The dot-dashed background arises from the final state $Z + jets$ where the missing E_t is generated by calorimeter resolution or by losing energy out of the end of the detector. The dotted background arises from the final state $t\bar{t}$ where there is an e^+e^- (or $\mu^+\mu^-$) pair of mass $M_Z \pm 20$ GeV and the missing E_T is due to neutrinos.

In order to make further improvement, the Higgs must be observed in the WW channel via the final state $\ell\nu + jets$ where there are a larger number of events. There are two sources of background, real W pairs arising from $q\bar{q} \rightarrow WW$ and the decay of $t\bar{t}$ pairs, and $W + jets$ from qg of gg initial states where the jet system has an invariant mass equal (within resolution) to the W mass. For large Higgs masses the most important source of Higgs bosons is the $qq \rightarrow qqH$ process (provided that the top quark is lighter than 175 GeV) and

hence the events have two quark jets in addition to the decay products of the Higgs. These jets are forward (see Figure 8) and have transverse momentum of order M_W. By contrast, the presence of such additional jets in the background is a higher order QCD effect and hence an additional suppression can be obtained by requiring their presence[23]. The requirement is more effective at eliminating the $W+jets$ rate (which occurs dominantly from qg initial states), than that the rate from $t\bar{t}$ decays (mainly from gg initial states) since gluons have a larger color charge and are more likely to radiate an extra jet. It is not yet clear that this final state can be observed, even with the forward jet requirement (tagging)[25]. However it is clear that the signal cannot be extracted without it.

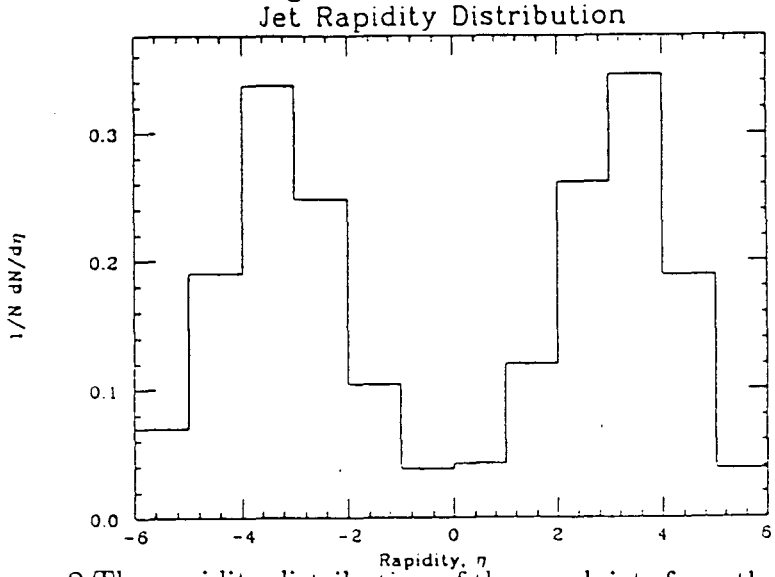

Figure 8 The rapidity distribution of the quark jets from the process $qq \to qqW$ at $\sqrt{s} = 17$ TeV. Figure from Ref. 24.

I will now make a few remarks about alternative models of weak interaction symmetry breaking. In models with supersymmetry[21], there are three neutral physical Higgs bosons and one charged one[26]. In these models the branching ratio of the neutral Higgs to WW or ZZ is reduced (recall that the Higgs self coupling, which controls the coupling of a Higgs to longitudinal W and Z bosons, does not increase with the Higgs mass) and hence the decay to $t\bar{t}$ can dominate. The signal in this channel is very difficult to extract due to the enormous background from $gg \to t\bar{t}$. If light enough the neutral Higgs may be observable via its $\gamma\gamma$ or $\tau\tau$ decay modes: the latter signal is enhanced over that

from a standard model Higgs.

The charged Higgs bosons in a supersymmetric model are easy to detect provided they are light enough to be produced in the decay of a top quark $t \rightarrow bH^+$ which is comparable in rate to $t \rightarrow Wb$. The H^+ will decay dominantly into $\tau\nu$ or $c\bar{s}$ and hence will give rise to an apparent violation of $e/\mu/\tau$ universality in top decays. Taus can be identified by their characteristic decay to a single pion and the $H \rightarrow c\bar{s}$ mode can be detected by looking at the invariant mass of dijet systems[27]. If the charged Higgs is too heavy to be produced in the decay of top, it must be produced from $q\bar{q} \rightarrow H^+H^-$ via an intermediate Z or γ. This is a rather small rate and detection of a charged higgs is now very difficult[28]. However, if low energy supersymmetry occurs in nature, its detection will occur in a hadron machine via the production of squarks and gluinos that occurs with a much larger rate and cleaner signature (see below).

In technicolor models[19], the Higgs is replaced by a scalar bound state of a new fermion-anti-fermion system. The dynamics is assumed to be similar to QCD and the Higgs boson is analogous to the pion of QCD. Such models predict new states analogous to the ρ and ω (ρ_t and ω_t)of QCD. These states have mass of order 1 TeV (the value is model dependent – it varies as $1/\sqrt{N}$ if the technigauge theory is SU(N)) and decay into final states of W and Z bosons. The ρ_t^0 can be searched for in the ZZ final state using the same methods as a standard model Higgs. The ρ_t^+ can be detected via its decay to WZ and thence to $\ell\nu\ell^+\ell^-$. Here the limiting factor is rate; for a ρ_t mass of 1.8 TeV ($N = 4$), the rate of excess WZ production 40 (10) fb at SSC (LHC) [29]. The ρ_t is a rather broad resonance ($\Gamma \sim 400$ GeV) and hence the signal is an excess of events rather than a sharp peak. The ω_t may be easier to observe: it appears as a sharp peak in the γZ final states[30]. This is shown in figure 9.

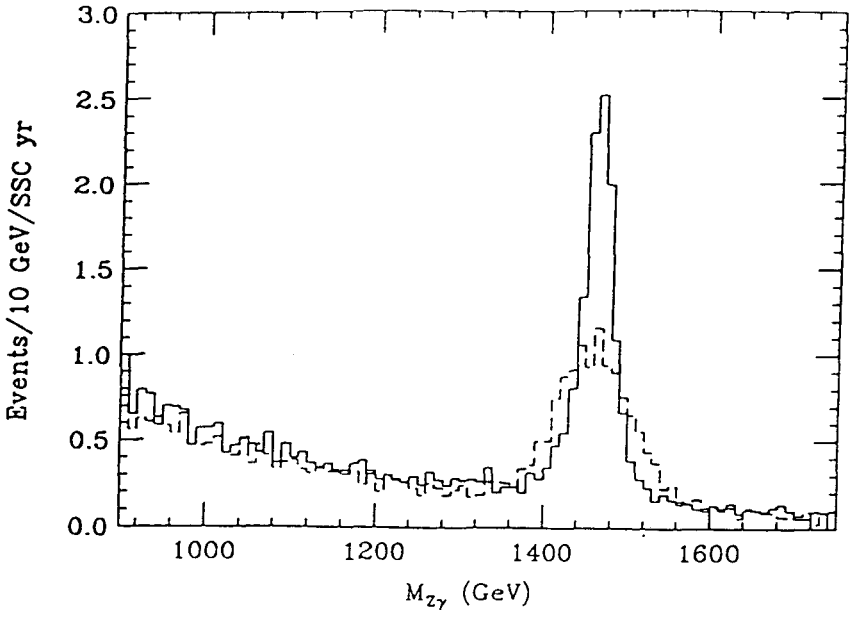

Figure 9 Detection of a ω_t of mass 1.46 TeV ($N = 6$) via its decay to $\gamma Z(\rightarrow e^+e^-, \mu^+\mu^-)$ at SSC. The electron peak is shown as a solid line, the muon peak as a dashed line. The sharper peak in the electron channel is due to the better resolution of SDC for electrons. Figure from Ref. 1.

The most difficult signal to detect is that in the so-called minimal strongly coupled standard model[31] where there are no degrees of freedom beyond those of the standard model and the coupling between longitudinally polarized gauge bosons (V_L) is large at high energy. In order to make predictions, one needs a model for this strongly coupled sector. There are several choices. One can take the low energy values of the $V_LV_L \rightarrow V_LV_L$ scattering amplitude and cut off the growth so that it saturates partial wave unitarity. For example the s-wave scattering amplitude for WW scattering at WW center of mass energy $\sqrt{s}$ is modeled as

$$a(W_L^-W_L^+ \rightarrow W_L^-W_L^+) = \frac{sG_F}{16\pi}\theta(16\pi G_F - s) + \theta(s - 16\pi G_F).$$

Alternatively, the low energy form of this amplitude can be unitarized using a K-matrix approach. A more dynamical model is to use the measured amplitude for $\pi\pi$ scattering which at low energy has the form

$$a(\pi^+\pi^- \rightarrow \pi^+\pi^-) = \frac{s}{32\pi F_\pi^2}$$

and rescale it by replacing F_π by $1/\sqrt{2G_F}$. Here one is assuming that the dynamics of weak symmetry breaking is the same as that of chiral symmetry breaking in QCD. Whichever model is used, the signals are the same: an excess of $V_L V_L$ events at large invariant mass over that predicted in the standard model with a light Higgs boson. The events have no sharp structure such as a peak at some value of the VV invariant mass. The best channel is W^+W^+ or W^-W^- since the standard model rates are small. Event rates for observing the W's in either the $e\nu$ or $\mu\nu$ with $p_t(e \text{ or } \mu) > 150$ GeV are 30 in 1 SSC yr for the unitarized model above[32]. The background is 6 events for the same cuts. Signals and backgrounds are uncertain since higher order QCD corrections are not known and hence rates are sensitive to the choice of Q^2. Since the event rates are small conclusions about the observability of the signal can depend on this choice.[32,33] This case is one where the extra energy of the SSC is a considerable advantage both in rate and signal/background. Signal (background) rates are approximately factor of 10 (3) greater at SSC.

The top quark.

It is quite possible that the top quark will be discovered at the Tevatron if its mass is below 180 GeV. Nevertheless the SSC or LHC must be able to detect it and measure as many of its properties as possible with the huge number of $t\bar{t}$ pairs that will be produced. Statistical errors on the the top mass measurement will be small compared to the systematic errors. There are three possible signatures for the detection of a top quark. First, the production of isolated $e\mu$ pairs (one each from the t and $\bar{t}$ in a $t\bar{t}$ event) has no background. However it one can only determine the mass of the top quark by assuming the standard decay modes and then using dependence of the production cross-section on the mass as predicted by QCD. Given the expected uncertainties of order 30% [34] on the cross-section expected from a fixed top quark mass, this method, while providing a very easy way to detect the top quark, is unlikely to be able to determine the mass within 20 GeV.

A second method involving only leptons is to look at the invariant mass of the two leptons of opposite charge arising from the semi-leptonic decays of the top and its daughter bottom quark. One selects events with an isolated electron and non-isolated muon of opposite charge that are close in phase space. Background arises from wrong combinations *e.g.* $t\bar{t} \to e^+ b\nu\bar{b}(\to \bar{c}(\to \mu^-\nu))u\bar{d}u\bar{d}$.

The correlation between the $e\mu$ mass and the top mass is used to extract the latter[35]. See figure 10. Here the main uncertainties on the extraction of the top mass are the b quark fragmentation function (the form used here was extracted from ALEPH[36] data) and the top p_t distribution. Since the top quark decays before it hadronizes into a top meson there is no top fragmentation function uncertainty. A determination of the top mass to better than 5 GeV seems possible using this mode.

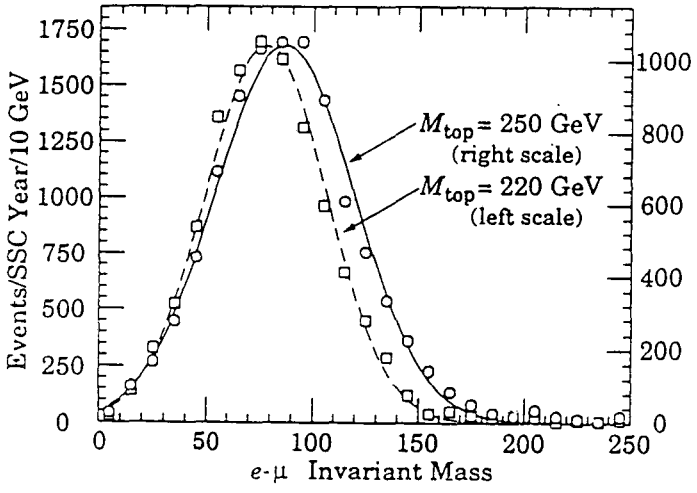

Figure 10 The invariant mass of an $e\mu$ pair of opposite charge for two different top quark masses. The electron must have $p_t > 40$ GeV and have less than 4 GeV of additional transverse energy in a cone of $\Delta R = 0.2$ around its direction. The muon must have $p_t > 20$ GeV and have more than 20 GeV of additional transverse energy in a cone of $\Delta R = 0.4$ around its direction. The transverse momentum of the $e\mu$ system must more than 120 GeV. Figure from ref 4 at SSC.

Finally one can attempt to fully reconstruct the decay $t \rightarrow bW(\rightarrow u\bar{d})$. Here events are triggered by requiring that the $\bar{t}$ decay semileptonically so as to produce an isolated e or μ. There is now a background from the final state $W(\rightarrow \ell\nu) + jets$. This background must be removed by requiring that there be at least one b quark in the event. This can be done by using a vertex detector to tag the decay[4] or by selecting events with a muon inside a jet[6] (from the semileptonic decay of b). The efficiency of the vertex tagging is expected to be

of order 10% in SDC [37]. One then searches for events where there are two jets with an invariant mass consistent with a W and then computes the invariant mass of the three jet system made up of these two jets and a third. The signal can be cleaned up further by requiring that this third jet be tagged as a $b-jet$ via the vertex system. The tag from the semileptonic b decay is less useful since then there is undetected energy carried off by the neutrino. Figure 11 shows the dijet invariant mass distribution. The requirement of two b-quarks in the event removes the background from $W+jet$ events. One now selects events around the W peak and combines this dijet system with one of the jets tagged as a b-quark (see figure 12). A peak is visible displaced somewhat below the mass of the top quark (250 GeV) used in the simulation[38]. The tail at large invariant masses is due to the wrong combination *viz.* $\bar{b}$ with W^- instead of $\bar{b}$ with W^+ since the sign of the b quarks cannot be determined from the vertex system. (The sign of the W is known by inference since the other W in the event decayed leptonically). The tail can be removed by requiring that the the b jet is close in phase space to the W[5] or that the charge is tagged by the semileptonic decay of the b quark[6].

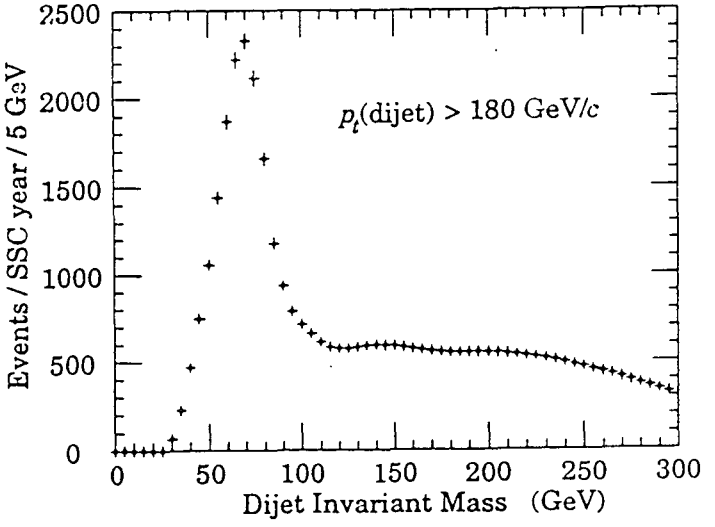

Figure 11 The dijet invariant mass distribution from $t\bar{t}$ events. The events have at least 4 jets with $p_t > 30$ GeV, and isolated e or μ with $p_t > 40$ GeV and at least two jets tagged as b-jets via the vertex system. Neither of the two jets in the dijet system can be one of the b-jets and the dijet system must have $p_t > 180GeV$. Figure from Ref. 4 at SSC.

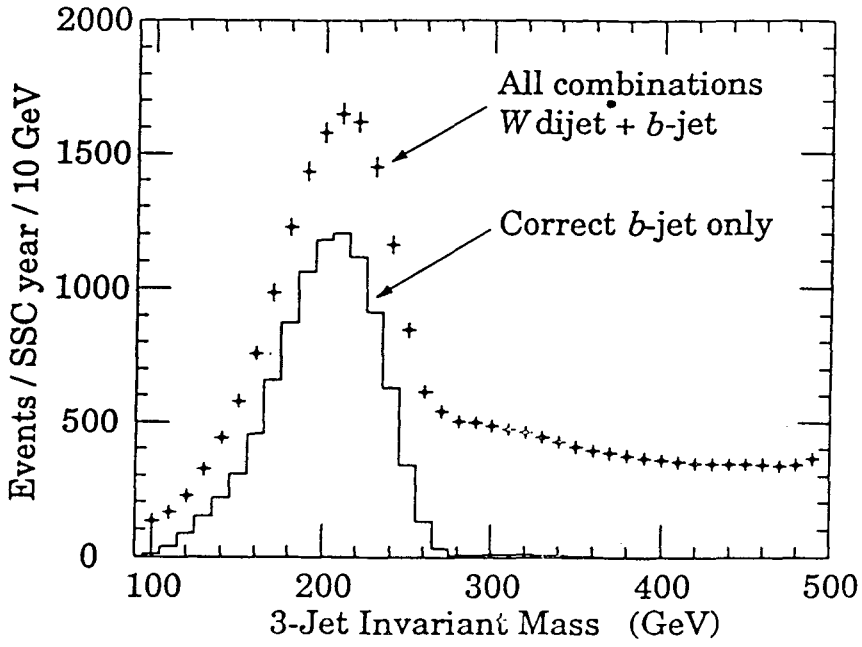

Figure 12 The three jet invariant mass distribution made of the dijets from Figure 11 having invariant mass between 50 and 95 GeV and a third jet tagged as having a b quark in it. Figure from Ref 4 at SSC.

The accuracy of the top mass determination is controlled by the ability to calibrate the jet energy scale accurately. The scale is affected by the intrinsic calibration and resolution of the calorimeter, but more important by the algorithm used to define a jet. Jets are usually defined using a fixed cone algorithm. Energy is collected in a cone of radius R (in $\eta - \phi$ space) around a jet core found by searching for the calorimeter cells with the most energy. Since jets have a finite size, some of their energy will fall outside the cone and not be measured. In addition some energy from the remainder of the event will fall into the cone. Since all of the three jets are in the same kinematic region and two of them reconstruct to the W one can use the W mass to calibrate the jet energy scale accurately. (There is some uncertainty since a b-jet may not look exactly like a light quark jet.) Using this technique the top mass could be measured to 5 GeV [38].

By comparing the event rates in the final states with $\ell + jets$, and 2 isolated leptons, one will be able to check universality in top decays and hence test for unusual decay modes. For example, if, as discussed above the top decays to

a charged Higgs which then decays dominantly to tau, the ratio of branching ratios $BR(t \rightarrow eX)/BR(t \rightarrow hadrons)$ will larger than expected in the standard model. As discussed above the tau decay mode can be searched for directly.

Gluino signals.

If low energy supersymmetry is the correct then one of the particles with the most copious production rate is the gluino. It is produced in pairs via $gg \rightarrow \tilde{g}\tilde{g}$. The signal depends upon the details of the supersymmetric model and in particular on the mass spectrum of other supersymmetric particles. If the squark is heavier than the gluino then the dominant decay modes of the gluino are expected to be $\tilde{g} \rightarrow q\bar{q}\xi^0$ or $\tilde{g} \rightarrow q\bar{q}\tilde{W}^+$. Here $\tilde{W}$ is the supersymmetric partner of the W and ξ is a weakly interacting "neutralino". ξ^0 may be stable or could decay $\xi^0 \rightarrow \xi'^0 q\bar{q}$. I shall give examples based on the decay chains $\tilde{g}\tilde{g} \rightarrow q\bar{q}\xi(\rightarrow q\bar{q}\xi')q\bar{q}\xi'$ and $\tilde{g}\tilde{g} \rightarrow q\bar{q}\tilde{W}(\rightarrow e\nu\xi')q\bar{q}\tilde{W}(\rightarrow e\nu\xi')$.

The former decay chain gives rise to as many as 6 jets and missing E_T carried off by ξ'. We assume a combined branching ratio of 10% for these decays[39]. There are three relevant sources of background in this channel: the final state $Z(\rightarrow \nu\overline{\nu}) + jets$, $t\bar{t}$ followed by semileptonic decays resulting in neutrinos that carry off energy, and a multi jet final state where the the missing E_t arises due to resolution or holes in the calorimeter. The last is the most difficult to simulate since it depends upon the tails of the jet resolution function. The resolution assumed by SDC is very non-gaussian and hence there are a large number of events where a jet is substantially mismeasured. Events of this type have the missing E_t closely aligned in azimuth with the mismeasured jet and can be eliminated by a cut on the azimuthal missing E_t direction. The $t\bar{t}$ and $b\bar{b}$ backgrounds are also substantial. They could be reduced somewhat by vetoing events where a lepton is detected. (This is not done here.) A cut on the circularity of the event defined by $C = 0.5min(\Sigma E_t \cdot \hat{n})^2\{\Sigma E_t^2\}$ $\hat{n}$ is a unit vector in the transverse plane and the minimization is with respect to its direction) is effective at reducing this background. It can be seen from Figure 13 that the signal stands clearly above all of these backgrounds for a gluino mass of 300 GeV. For larger masses, the rate becomes less but the missing E_t and the jet energies become larger and the signal to background ratio improves.

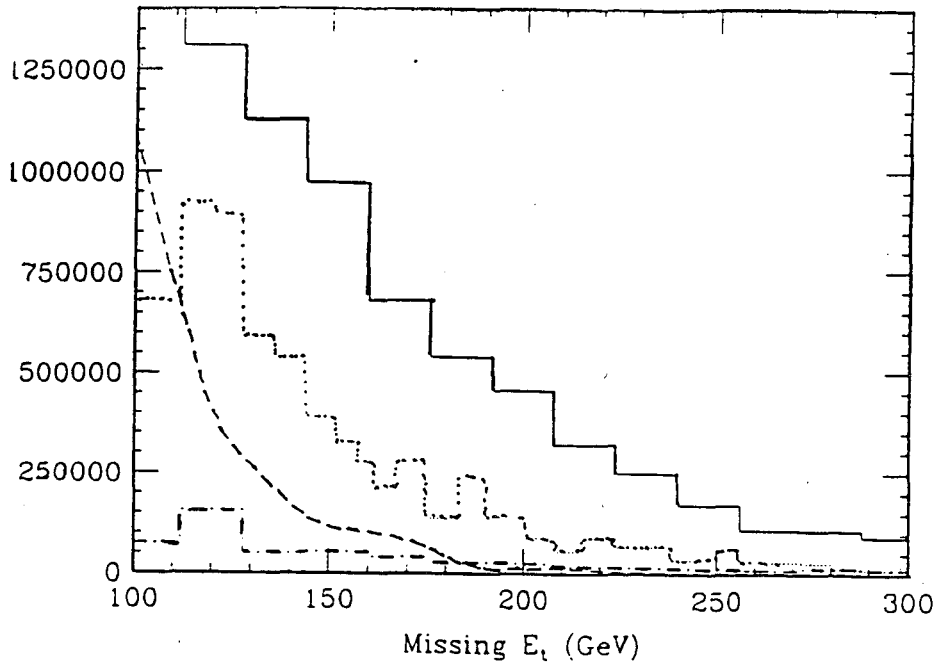

Figure 13 The distribution in missing E_t arising from the production of a pair of gluinos of mass 300 GeV (solid histogram, see text). Events are required to have at least 3 jets with $E_T > 70$ GeV and to be separated from each other by $\Delta R > 0.7$. Events are rejected if they contain a jet within 20° in azimuth of the missing E_t direction and if they have circularity of more than 0.2. The dashed curve arises from multijet final states where energy is lost out of the end of the detector (assumed to cover $|\eta < 5|$) or appears due to mismeasurement of jet energies. The SDC resolution is used. The dashed background is from the $t\bar{t}$ and $b\bar{b}$ final states. The dot-dashed is from $Z(\rightarrow \nu\nu) + jets$. Figure from Ref. 40.

It will be difficult to determine the gluino mass from the jets+ missing E_t final state. The mass cannot be inferred from the event rate since the branching ratios are not known *a priori*. The alternate decay mode leads to a final state of two leptons and some jets. Background is least if the leptons are required to have the same sign. This is shown in Figure 14. The peak in the invariant mass distribution shown is sensitive to the gluino mass and can be used to determine that mass to within 10%.

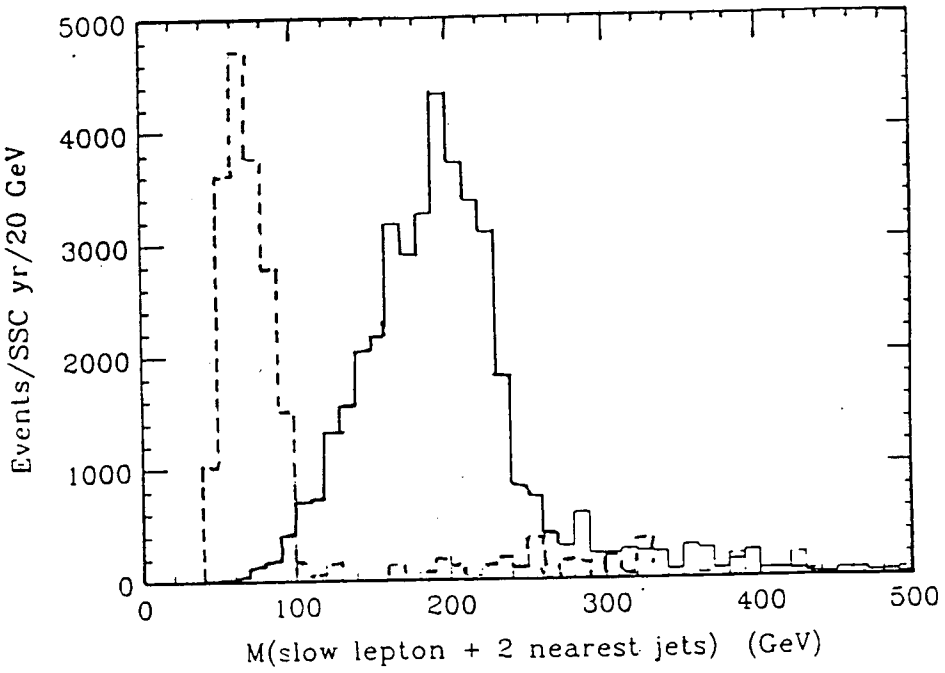

Figure 14 Events at SSC are selected that have at least 4 jets with $p_t > 50$ GeV and two isolated leptons (e or μ) of the same sign and either both having $p_t > 20GeV$ or one having $p_t > 40$GeV and the other having $p_t > 15$ GeV. The event rate is shown as a function of the invariant mass of the lepton with lower p_t and the two jets that are closest to it in $\eta - \phi$ space. The solid histogram shows the distribution from gluino pair events where a combined branching ratio of 1% and a gluino mass of 300 GeV were assumed. The dashed histogram is from $t\bar{t}$ ($m_t = 150$ GeV) events where the leptons are *not* required to be isolated. An isolation requirement eliminates this background since at least one of the leptons must arise from charm or bottom decay. Figure from ref 40.

Conclusions.

In terms of the physics capabilities and SSC operating at $10^{33}cm^{-2}sec^{-1}$ and $\sqrt{s} = 40$ TeV is broadly equivalent to an LHC operating at $10^{34}cm^{-2}sec^{-1}$ and $\sqrt{s} = 16$ TeV. But there are some important differences. For the production of particles of mass less than 100 GeV or so, the LHC has a larger rate since for this range of masses the production cross-sections do not grow very rapidly with energy. By contrast, for heavy particles such as the production of gauge boson pairs of invariant mass greater than 1 TeV, the SSC has an advantage due

to more rapid growth of the cross-section with energy. For processes involving leptons at low transverse momentum ($\lesssim$20 GeV), where the leptons have to be isolated in order to reject background from bottom and charm decays, pile up of minimum bias events at the higher luminosity can lead to a loss of efficiency.

The requirements placed on a 4π optimised for the search for new physics at large p_t detector are by now clear. Good acceptance (at least $|\eta| < 2.5$) for electrons (calorimeter and tracking combined) and muons with a momentum resolution better than 10% for $p_t < 500$ GeV is adequate. Some method of determining the sign of electrons is very useful in reducing some backgrounds as in the gluino example discussed above. There will be rather few leptons with p_t larger than this unless, there is new gauge boson of large mass in this case the electromagnetic calorimeter can be used to accurately measure the mass of such a particle in the decay to electrons. If one wants to measure the mass in the muon decay mode a very sophisticated muon system will be needed[6].

The calorimeter must cover $|\eta| < 5(4.5)$ at SSC (LHC) in order to provide good enough missing E_t resolution to be able to search for gluinos and $H \rightarrow \ell\ell\nu\nu$. In the central region ($|\eta| < 3$), segmentation of 0.05×0.05 in $\eta - \phi$ space and a jet resolution of $50\%/\sqrt{E(GeV)} + 3\%$ are adequate. Provided that these are achieved the dominant uncertainty on the jet energy measurements (and on the ability to reconstruct objects decaying to jets) will arise from clustering effects such as those discussed above[41].

The resolution of the electromagnetic calorimeter is driven by the need to extract the $H \rightarrow \gamma\gamma$ signal. As discussed above, by selecting events that also contain a W (tagged by its leptonic decay), extraordinary resolution may not be needed.

I have concentrated in this talk on high p_t physics. There will be much physics at SSC/LHC that is not of this type. In particular the production cross-section for b quarks is enormous ($\sim 0.1mb$). It is not yet clear whether the 4π detectors can exploit this huge sample of $b's$ or whether a dedicated collider or fixed target b experiment will be needed.

References.

1) Expression of Interest submitted by the SDC collaboration to the SSC Laboratory June 1990.

2) Expression of Interest submitted by the EMPACT collaboration to the SSC Laboratory June 1990.

3) Expression of Interest submitted by the L* collaboration to the SSC Laboratory June 1990.

4) Letter of Intent submitted by the SDC collaboration to the SSC Laboratory December 1991.

5) Letter of Intent submitted by the EMPACT collaboration to the SSC Laboratory December 1991.

6) Letter of Intent submitted by the L* collaboration to the SSC Laboratory December 1991.

7) Proceedings of the Aachen LHC workshop, CERN-90-10.

8) R. W. Brown and K.O. Mikaelian *Phys. Rev.* **D19**, 922 (1979), J. Owens and J. Ohnemus FSU-HEP-901212 (1990), B. Mele P. Nason and G. Ridolphi CERN-TH-5890 (1990).

9) E. W. N. Glover and J.J van der Bij. *Phys. Lett.* **B219**, 488 (1989).

10) R.M. Barnett, K. Einsweiler and I. Hinchliffe, SSC-SDC-90-00099, LBL-30247

11) R.K. Ellis *et al. Nucl. Phys.* **B297**, 221 (1988).

12) L. Di Lella, ref 7.

13) R. Ansari *et al. Zeit. fur Physik* **C41**, 395 (1988).

14) CDF collaboration reported by R. Blair ANL-HEP-CP-89-07.

15) M. Mangano, SSC-SDC-00113 (1990).

16) J. Gunion UCD 91-2, W.J. Marciano and F.E. Paige, BNL preprint (1990).

17) For a review see M. Lindner *Zeit. fur Physik* **C31**, 295 (1986).

18) For a review see I. Hinchliffe *Ann. Rev. Nucl. and Part. Sci.* **36**, 505 (1986)

19) For a review see E. Farhi and L. Susskind *Phys. Rep.* **74**, 277 (1981).

20) U. Baur and E. W.N. Glover MAD-PH-577 (also in ref 7.)

21) I. Hinchliffe, SDC-90-00100.

22) T. Hessing and S. Behrends, "Inclusive Jet Spectrum E_t Corrections and Resolution Unsmearing", CDF internal note 1132.

23) R. Kleiss and W.J. Stirling *Phys. Lett.* **200B**, 193 (1988).

24) M.H. Seymour, in ref 7.

25) D. Froidervaux in ref 7.

26) For a detailed discussion of these signals at LHC see Z. Kunszt and F. Zwirner in ref 7.

27) R.M. Barnett *et al.*SSC-SDC-90-00141, LBL-29774.

28) J.F. Gunion *et al.* in *Experiments, Detectors and Experimetnal areas for the SSC* Ed. R. Donaldson and M.D. Gilchriese, World Scientific (1987).

29) E. Eichten *et al. Rev. Mod. Phys.* **56**, 579 (1984).

30) M. Mangano, SSC-SDC-

31) M.S. Chanowitz and M.K. Gaillard *Nucl. Phys.* **B261**, 379 (1985).

32) M Berger and M. Chanowitz, LBL-30476 (1991).

33) V. Barger *et al. Phys. Rev.* **D42**, 3052 (1990).

34) G. Altarelli *et al. Nucl. Phys.* **B308**, 724 (1988).

35) A. Barbaro-Galtieri *et al.* SSC-SDC-90-00038.

36) D. Decamp *et al. Phys. Lett.* **B244**, 512 (1990).

37) B. Hubbard SDC-90-00031.

38) R.J. Hollebeek *et al.* SSC-SDC-90-00117, SSC-SDC-90-00118.

39) H. Baer, X. Tata and J. Woodside *Phys. Rev.* **D41**, 906 (1990).

40) "Reply by the Solenoidal detector collaboration to questions from the SSC PAC", SDC-90-00084 (1990).

41) This issue is discussed in detail in refs 4-6. See also R. Blair *et al.*SSC-SDC-90-00150 and A. Para *et al.*SSC-SDC-90-00149.

LAWRENCE BERKELEY LABORATORY
UNIVERSITY OF CALIFORNIA
INFORMATION RESOURCES DEPARTMENT
BERKELEY, CALIFORNIA 94720